



Ovarian Stimulation Altered Uterine Fluid Extracellular Vesicles miRNA Affecting Implantation in Rats

Xi Huang^{1,2} · Jing Zhao^{1,2} · Qiong Zhang^{1,2} · Yonggang Wang^{1,2} · Yanping Li^{1,2}

Received: 29 May 2023 / Accepted: 18 December 2023 / Published online: 12 January 2024
© The Author(s), under exclusive licence to Society for Reproductive Investigation 2024

Abstract

Uterine fluid (UF) extracellular vesicle (EV) miRNA may affect implantation and could be the potential biomarker of endometrial receptivity (ER). Ovarian stimulation (OS) could damage the ER but its mechanism is still unclear. Here, we evaluate the affections of OS on UF EV miRNA expression and implantation. Female rats were divided into three groups: natural cycle or injection with GnRH-a following HP-HMG or u-FSH. UF was collected on the 5th day of gestation. Affinity membrane columns were utilized to isolate EVs from UF, obtained during implantation flushing. The EV miRNAs were sequenced, and five of them were validated by qRT-PCR. HTR-8/Svneo cells were transfected with miR-223-3p mimic and inhibitor, followed by conducting colony formation, invasion, migration, and adhesion assays to assess the cellular functions. In OS groups, the implantation rate decreased ($p < 0.05$), and the pinopode was damaged in the OS groups. The EVs were isolated from UF, and the differential expression key miRNAs were involved in several regulation pathways, such as cancer, endocrine, and cell cycles, which were correlated with ER and implantation. Among the miRNAs, miR-223-5p greatly differed and was most consistent with the sequencing results, followed by miR-223-3p and miR-98-5P. miR-223-3p promoted HTR-8/Svneo cells grow and ability of invasion, migration, and adhesion. OS altered UF EVs miRNAs affecting implantation in rats, and miR-223-3p might be the key molecule.

Keywords Ovarian stimulation · Uterine fluid · Extracellular vesicle · MicroRNA · Endometrial receptivity

Introduction

When an embryo triggers, the endometrium should transfer into a receptive status; otherwise, the implantation fails [1]. This spatial and temporal shift of the endometrium is referred to as endometrial receptivity (ER) and the window of implantation (WOI) During this period, endometrial epithelium and stromal cells would go through a series of differentiation to become embryo receptable. A retrospective study found no significant increase in the implantation rate or lower biochemical pregnancies in pre-implantation genetic testing cycles [2], indicating that compromised ER

may have a more detrimental impact on implantation than active embryo stages or genetic abnormalities.

By unraveling the mysteries of female fertility physiology, ovarian stimulation (OS) therapy has been extensively developed, significantly enhancing the clinical efficiency of artificial reproduction technology (ART). Regrettably, it also damages ER. After OS therapy, the elevated progesterone level could advance turn on WOI [3]; pinopode and endometrial epithelial nucleoli decreased [3, 4]; proteomics and functional genomics undergo alterations [5].

The uterine fluid (UF), the microenvironment during implantation, performs a crucial role p not only as a liquid medium connecting the floating embryo and endometrium but also information transporter. The general condition of UF, such as appropriate pH, osmotic pressure, and volume, affects the implantation, and its secret omics showed that UF can reflect a mother's readiness for pregnancy [6]. In 2008, extracellular vesicle (EV) was first isolated from mice UF, also known as uterosome [7]. EV is a nanoscale vesicle surrounded by a double membrane with transmembrane protein, containing nucleic acids, proteins, and lipids. EVs

✉ Yanping Li
liyanyan@csu.edu.cn

¹ Department of Reproductive Medicine, Xiangya Hospital, Central South University, NO.87, Xiangya Road, Kaifu District, Changsha, Hunan, China

² Clinical Research Center for Women's Reproductive Health in Hunan Province, NO.87, Xiangya Road, Kaifu District, Changsha, Hunan, China

were found under the electron microscope for the first time in 1985 [8]. Nowadays, EVs have been found in body fluids and culture supernatants of virtually every type of cell. By analyzing the cargo and tracking their movements, EVs are considered to be a novel mode of intercellular communication. EV can be roughly categorized into three subgroups based on their formation: exosome, microvesicle (MV), and apoptotic body. Both exosomes and MV have been proven to play a role in intercellular communication, liquid biomarkers of the disease, and drug carriers. Studies on EVs covered the field of reproductive cavity biological fluid, including the epididymis, semen, follicular fluid, oviductal luminal fluid, vaginal fluid, UF, and culture medium such as the embryo and endometrial epithelial cells [9–12]. The contents, mainly small RNA and protein, carry real-time information to recipient cells or tissues. Besides, exogenously supplying UF EVs could improve embryo implantation. The protein-enriched UF EVs play a vital role in embryo implantation. Among them, MEP1B transferred by UF EVs to trophoblast cells could promote trophoblast cell proliferation and migration [13]. Consequently, UF EVs are very important in regulating the implantation process at the maternal–fetal interface through bilateral targeted crosstalk between endometrium and embryo.

We analyzed the alteration of UF EVs miRNA expression of OS rats during implantation. We are eager to expand our knowledge of the relationship between OS and implantation, and identify potential miRNA candidates for further mechanism research, ultimately aiming to discover a novel, effective, and noninvasive ER liquid markers in the future.

Materials and Methods

OS Animals

Specific pathogen-free female Sprague–Dawley (SD) rats aged 7 weeks, and SD male rats aged 8–10 weeks, were purchased from the Department of Laboratory Animal, Central South University, Changsha, Hunan, China. No experiment or drug was conducted. The rats were housed in a clean barrier environment, characterized by temperature of 24 ± 2 °C, a relative humidity of $50\% \pm 5\%$, continuous lights for 12 h (from 6:00 am to 18:00), free access to food and water, a maximum of 3–4 rats per cage, and daily bedding materials changes. After a 5-day adaptation period, vaginal smears were observed to determine the estrous cycle and efficiency of OS treatment (Fig. 1A). Rats exhibiting incomplete estrous cycles, too-deep pituitary suppression, hyperstimulation, and failed mating were excluded.

GnRH-a/HP-HMG/HCG (group M) and GnRH-a/u-FSH/HCG (group F) were used to generate OS rats. Gonadotropin-releasing hormone agonist (GnRH-a, Ferring, Denmark)

was administered intraperitoneally at a dosage of 4 µg per 250–300 g body weight daily at 9 am starting from the post-estrus period. High-purity hMG (HP-hMG, MENOPUR, Ferring) or u-FSH (Livzon, China) was injected intraperitoneally at a dosage of 40 IU per 200 g body weight on day 7 of downregulation. HCG was administered intraperitoneally at a dosage of 1050 IU per 200 g body weight 48 h following gonadotropin injection. The rats in the natural cycle group (group NC) were administered an equal volume of 4 °C saline at the same time. Male and female rats were caged 1:2 on the day of HCG administration, and rats with vaginal plug or sperm were marked Pd1 (Fig. 1B) on the following morning. We collected ovaries, uterus, and UF at Pd5 (Fig. 1E).

UF EVs Isolation and Identification

UF was centrifugated at 4 °C, 10,000 *g* for 30 min, and filtered through a 0.22-µm filter (Millipore). Due to the limited quantity of EVs isolated from a single rat's UF, we combined the UF samples of six rats to obtain a sufficient quantity for subsequent experiments. The combined UF sample was concentrated using ultrafiltration concentration tubes (Millipore, 100KD). Filtered solution was collected as negative control for the western blot. Membrane affinity spin column (QIAGEN, exoEasy Maxi Kit) was used to isolate EVs from the concentrated liquid following the standard protocol in the exoRNeasy Midi Kit Handbook and UF EV elute was diluted 5 times by 0.22 µm filtered PBS. The transmission electron microscopy (TEM) was used to identify the morphology, performed at the Laboratory of Biomedical Electronic Microscopy Higher Research Center, Central South University. The particle distribution was analyzed with dynamic light scattering (DLS) using Zetasizer Nano ZSP instrument (Malvern). Specific surface protein markers, CD63 (1:500, Rabbit#25682–1-AP, Proteintech) and TSG101 (1:1000, Rabbit# ab109201, Proteintech), were characterized by the western blot. All characterization tests had been conducted triplicates.

Cell Line and Cell Culture

To investigate the function of miR-223-3p on embryo implantation, we selected the HTR-8/SVneo and Ishikawa cell lines representing trophoblasts and endometrial cells [14, 15], respectively, to conduct a series of cellular functional assays and adhesion assay that intimate the implantation process [16]. The Ishikawa cell line was purchased from National Infrastructure of Cell Line Resource. The HTR-8/SVneo cell line was kindly gifted from the Obstetrics and Gynecology Lab of Xiangya Hospital, Central South University. Ishikawa cells were cultured

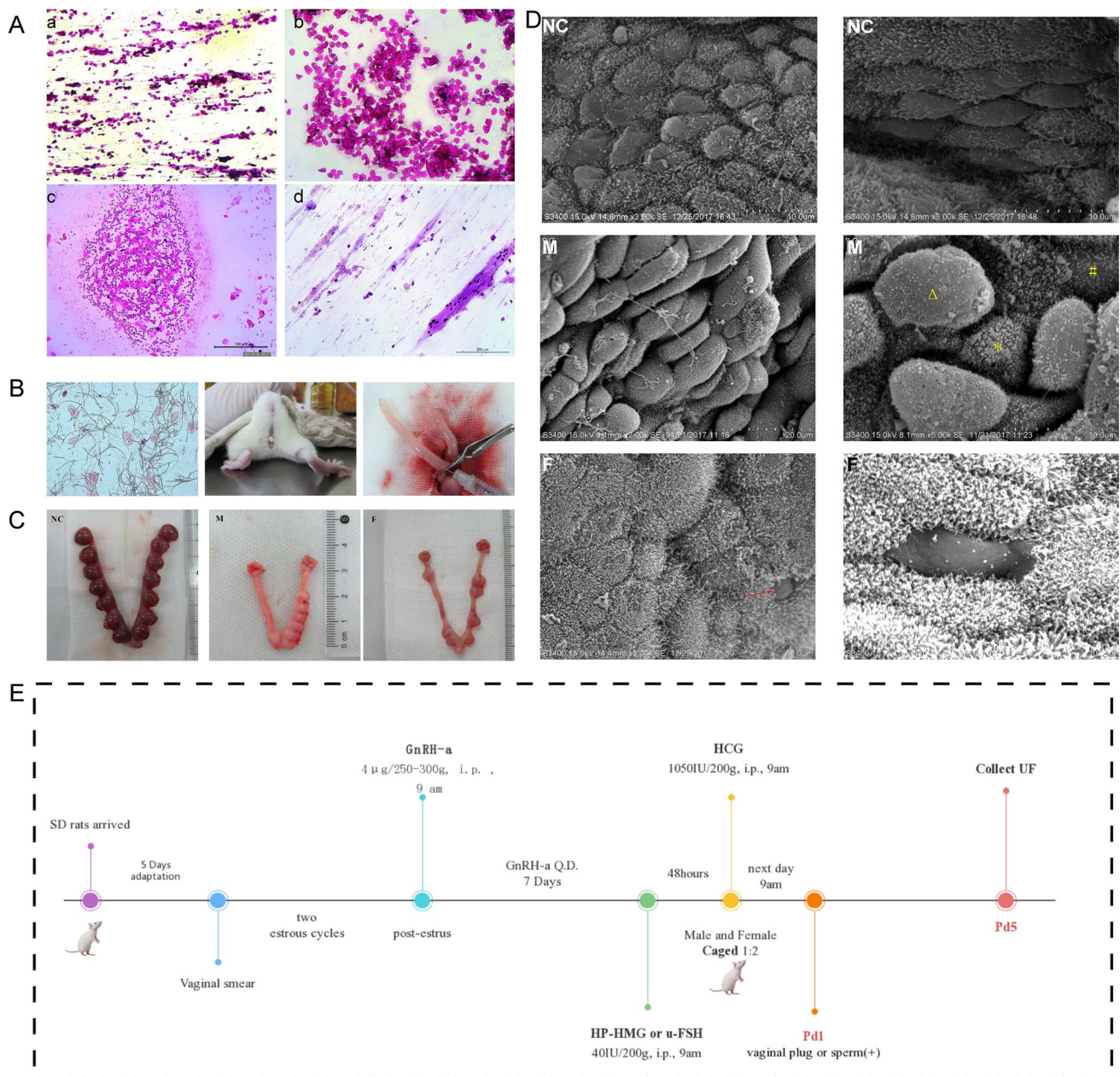


Fig. 1 OS rat implantation damaged. **A** Vaginal smears were stained with HE to determine OS treatment Rats' estrous cycle and efficiency. a-d were proestrus, estrus, metestrus, and diestrus interval; **B** Sperm, vaginal plug, and UF collection; **C** OS rats showed fewer embryos; **D**

Expression of pinopode. Δ fully developed pinopode; # early developing pinopode; * underdevelopment pinopode; **E** Timeline of the rats' OS cycle and sampling

in DMEM/F-12 (Gibco, USA, 11965092), containing 5% fetal bovine serum (FBS) (Gibco, USA, A4766801); HTR-8 cells were cultured in RPMI 1640(Gibco, USA, 12633012) containing 4% FBS. One percent penicillin–streptomycin (10,000U mL) (Gibco, USA, 15140122) was added intermittently. Cells were cultured at a 37 °C, 5%CO₂ temperature cell incubator. Cell medium exchanges were performed every 2 days.

HTR-8/Svneo Cells Transfected miR-223-3p Mimic and Inhibitor

miR-223-3p mimic and inhibitor were obtained from Ribo Technology, China. The INVI RNA DNA reagent (Invigentech, USA, IV1216300) was utilized to transfect siRNA into HTR-8 cells. When HTR-8 cells' culture reaches to 70%, the siRNA and INVI reagent were mixed at a 1:1 ratio and incubated for 20 min at room temperature. Subsequently, the

mixture was gently blown to mix well and added to the cell culture medium. Then, HTR-8 cells were transferred to an incubator for 24 h. The INVI mixture was discarded, and the cells were switched to a normal complete culture medium.

Colony Formation

Transfected HTR-8/Svneo cells in the logarithmic growth phase were seeded at a density of 1000 cells per well in 6-well plates. Culture medium was exchanged every 2 to 3 days and counted the number of cell colonies after approximately 15 days of culture.

In Vitro Migration/Invasion Assays

In vitro invasion and migration were performed 48 h after siRNA infection of HTR-8/Svneo cells, using the Transwell system (0.8 μm , Corning, USA, 3422). Prior to the invasion assay, the 24-well Transwell system was frozen with a 200 μL tip at $-20\text{ }^\circ\text{C}$; Matrigel (Corning, USA, 34,532) was diluted to 0.6 mg/mL in RPMI 1640, and 100 μL was added to the chamber and incubate at $37\text{ }^\circ\text{C}$ for 30 min. A cell suspension of 1.0×10^4 cells was suspended in 100 μL RPMI 1640 and implanted in the chamber. The lower well contained 600 μL RPMI 1640 with 1% FBS. After a 24-h incubation at $37\text{ }^\circ\text{C}$ and 5% CO_2 , the medium from the chamber and lower well was aspirated. The chamber was washed twice with PBS, followed by fixation with 4% polyformaldehyde at room temperature for 20 min. The chamber was again washed twice with PBS, and 1% crystal violet (v/v) (Beyotime, China, C0121) was used to stain at room temperature for 3–5 min. The crystal violet was washed out with PBS, and the surface cells were removed using a small cotton swab. The number of invasion cells was counted at $200\times$ original magnification. The migration assay was nearly identical to the invasion assay, except without the Matrigel coating.

Cell Adhesion

The HTR-8/Svneo cells were cultured with 5000 cells in 100 μL RPMI1640-4%FBS within a 96-well low adhesion transparent round plate (Corning, USA, 7007). The incubation was conducted at $37\text{ }^\circ\text{C}$ and 5% CO_2 for an overnight period. Concurrently, Ishikawa cells were seeded with 5×10^5 cells in 100 μL DMEM-5%FBS in an adjacent well of the same plate and incubated overnight. The following day, HTR-8 cells formed trophoblast spheres, while Ishikawa cells developed a layer resembling the endometrium interface during embryo implantation. The trophoblast spheres were subsequently aspirated and transferred onto the Ishikawa cell layer. The number of spheres post-implantation was enumerated. Subsequently, the plates

were incubated for an additional 24 h in DMEM-5%FBS medium at $37\text{ }^\circ\text{C}$ and in a CO_2 concentration of 5%. Unattached trophoblast spheres were removed by gently shaking the plate at a speed of 70 rpm for approximately 5–10 min. Ultimately, the remaining attached spheres were counted to determine the adhesion rate (%), which was calculated by dividing the number of spheres after washing by the initial number of implanted spheres.

RNA Isolation, miRNA Sequencing, and Bioinformatics Analysis

According to the standard protocol of the exoRNeasy Midi Kit and miRNeasy Micro Kit Handbook (QIAGEN 77064), EVs captured in the exoEasy Maxi Spin Columns were directly lysed in the affinity membrane with QIAzol. Sequencing samples were sent to RiboBio. (Guangzhou, China) for quality assessment and following the microRNA sequencing. We compared the UF EV miRNA expression among each group. The target genes of candidate miRNA were predicted from four databases: TargetScan, miRDB, miRTarBase, and miRWalk. Biological pathway was analyzed based on Kyoto encyclopedia of genes and genomes (KEGG) databases. Each target gene's functional annotations were analyzed based on databases Gene Ontology (GO).

miRNA Validated by qRT-PCR

Purity and concentration of the total RNA were assessed using a Nanodrop 2000 Ultramicro spectrophotometer (Thermo Scientific). Quantitative reverse transcription–polymerase chain reaction (qRT-PCR) was performed to validate the expression of 5 selected miRNAs after comparing the miRNA profiles. This experiment was conducted using miScript SYBR Green PCR Kit (QIAGEN 218073) according to manufacturer's instructions. Briefly, nearly 50 ng RNA was reverse transcript to cDNA using miScript II RT Kit (QIAGEN 218160). qRT-PCR experiment was conducted using ABI ViiA™ 7 (Thermo) with manufacturer's instrument. A 10 μL PCR reaction was used including 5 μL QuantiTect SYBR Green PCR Master Mix, 1 μL miScript Universal Primer, 1 μL miScript Primer Assay, Template cDNA, and RNase-free water. Considering the miRNA proportion of sRNA in the UF EVs is very small (Fig. 3A) and EV miRNA housekeeping genes remains uncertain [17], the comparative CT ($2^{-\Delta\text{CT}}$) was used to calculate the relative quantitative of selected miRNA expression for common endogenous genes U6[18] (Table 1).

Table 1 Primers used in q RT-PCR analysis

miRNA	Sequence	ID
rno-miR-199a-5p	CCCAGUGUUCAGACUACCGUUC	MIMAT0000872
rno-miR-340-5p	UUAUAAAGCAAUGAGACUGAUU	MIMAT0004650
rno-miR-223-3p	UGUCAGUUUGUCAAAUACCCC	MIMAT0000892
rno-miR-223-5p	CGUGUAUUUGACAAGCUGAGUUG	MIMAT0017165
rno-miR-98-5p	UGAGGUAGUAAGUUGUAUUGUU	MIMAT0000819
rno-U6-F	CTCGCTTCGGCAGCACA	NM_001359042.1
rno-U6-R	AACGCTTACGAATTTGCGT	

Statistical Analysis and Image Processing

Data were recorded as mean \pm standard error. Statistics were processed by SPSS22.0. *t*-test, Wilcoxon rank sum test, least-significant difference test, and Kruskal–Wallis test. *p*-values were both bilateral, the test level was $\alpha = 0.05$, and the calibration was necessary. Images were processed using GraphPad Prism 7 and Image-Pro plus 6. An alphabetical notion was used to mark the statistical difference. In the same table or figure, values with different lowercase superscripts indicate a significant difference ($p < 0.05$), and capital letter superscripts indicate significant difference ($p < 0.01$).

Results

OS Rats' Implantation and Pinopode Damaged

Vaginal smears stayed in the diestrus since the fourth day of GnRH-a administration and turned to the estrus currently with sexual arousal after gonadotropin injection. OS groups had bigger ovary. The pregnancy rate and average number of embryos were significantly decreased in OS groups (Fig. 1C). The development of pinopode was categorized into three stages: developing, fully developed, and regressing [19]. In this study, group NC showed developing pinopode: characterized by a diminished density of microvilli, the appearance of woolens and flattened membrane protuberances on the endometrial surface was observed; group M showed a fully developed pinopode but desynchrony: early development and underdevelopment existed at the same microscopic field. Group F showed occasional pinopode and densely erecting microvilli (Fig. 1D).

Both Exosomes and MVs Existed in UF

The size distribution exhibited two peaks at 59.56 nm and 258.5 nm, accounting for 14.5% and 85.5% of the particles, respectively. These sizes covered the range of both exosome and MVs. CD63 and TSG-1 were positively stained. Both exosomes and MVs presented in the UF

sample under TEM: exosome showed a typical cup shape and MV showed rounded electron dense with double membrane structure (Fig. 2).

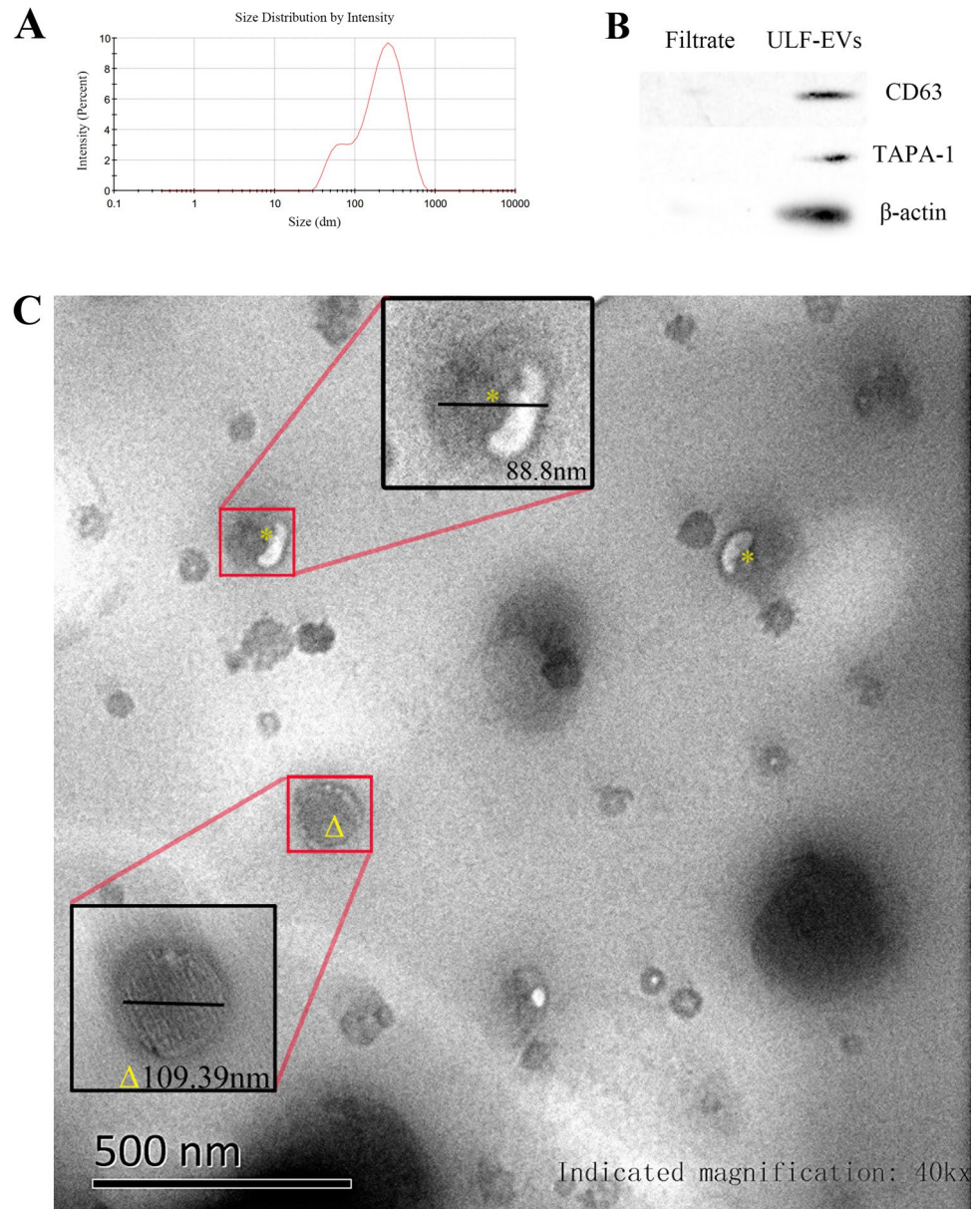
Altered UF EVs miRNA Expression

The common sequences of three groups were only 5.09%. Based on the original hierarchical clustering analysis, groups M1 and NC3 exhibited poor repeatability; therefore, they were excluded and the optimized result was presented in Fig. 3B; group F showed low expression, and groups M and NC were clustered, which was consistent with the developmental stage of the pinopode. According to the standard cutoff, *p*-value of < 0.05 , fold change > 2 , and 10 miRNAs were found to be upregulated and 11 miRNAs downregulated in group M compared with group NC; 47 miRNAs were downregulated in group F compared with group NC, and 14 of them were also downregulated compared with group M (Fig. 4). Co-expressed miRNAs were selected from the three groups, excluding those with poor repeatability based on the cluster analysis. Finally, 30 candidate miRNAs were selected, and a total of 4584 target genes were predicted (Fig. 3; SRA accession: PRJNA602111; Supplement Table 1).

KEGG Pathways and GO Analysis

With corrected *p*-value < 0.01 , 60 biological signaling pathways were selected according the KEGG database. Metabolic pathways involved majority of target genes. Endocrine-related pathways, such as estrogen, progesterone-mediated, prolactin, and GnRH, were also found. In addition, cell cycle, endocytosis, hippo signaling pathway, and cancer pathways are also related with implantation. From the concentration of GO annotation, the most significant molecular functions are protein binding and catalytic activity, and the cellular component is partly intracellular, and the biological process is cellular, single organism, and metabolic process (Fig. 3, Supplement Table 2).

Fig. 2 Identification of UF EVs. **A** DLS showed the particle size distribution had two peaks of 59.56 nm and 258.5 nm accounting for 14.5% and 85.5%. **B** Western blots showed that both CD63 and TSG101 in UF EVs were positive. **C** TEM showed two types of EVs. * Cup-like vesicle with diameter 88.8 nm, consistent with characters of exosome. Δ larger vesicle, 109.39 nm, showed a rounded electron dense with membrane structure, consistent with characters of MV



Validation for the Robustness of the miRNA Sequencing

The following key miRNAs, rno-miR-223-3p, rno-miR-223-5p, rno-miR-340-5p, rno-miR-98-5p, and rno-miR-199a-5p were selected for qRT-PCR validation according to studies on disease biomarkers and reproduction [20–23]. Among these miRNAs, rno-miR-199a-5p, and rno-miR-340-5p showed no difference in expression across the three groups. The expression of rno-miR-223-3p, rno-miR-223-5p, and rno-miR-98-5p in group M was highest. Rno-miR-223-3p demonstrating a statistically significant increase in group F compared to group NC, where rno-miR-223-5p and rno-miR-98-50 showed no differences. Although the expression of candidate miRNAs in group F

was lowest in sequencing, their expression was higher than in group NC in the qRT-PCR validation experiment. Considering that the abundance of miRNA was low, Pearson's correlation was separately analyzed between qRT-PCR validation and sequencing between groups OS and NC, to reduce experimental errors, and results indicated that the correlation in groups M and NC was acceptable, while no correlation was observed between groups F and NC. The concentration of EVs and miRNAs was assumed to be low in UF and frozen could also be harmful [24]. In conclusion, miR-223-5p was found to be the best fit, followed by miR-223-3p and rno-miR-98-5p. miR-223-3p showed the most significant disparity among three groups. Three common target genes were identified: Ankrd17, Col13a1, and Stk39 (Fig. 4).

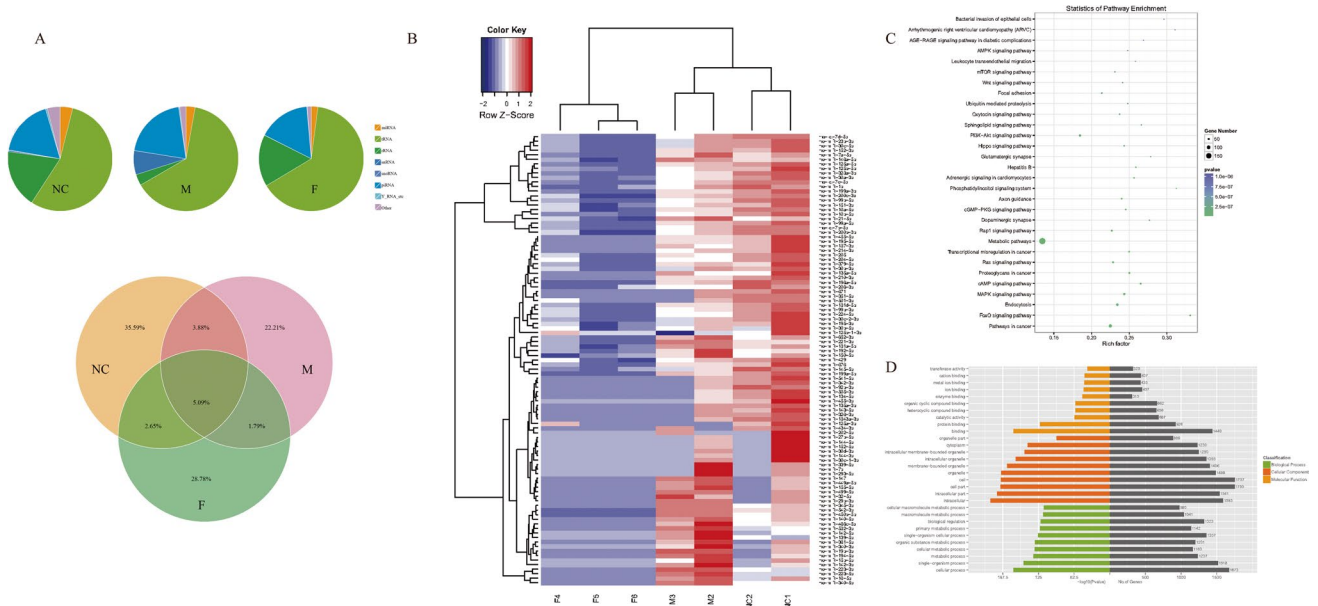


Fig. 3 MiRNA expression profiles altered. **A** miRNA proportion of sRNA in each group and Venn chart showed common sequences and the endemic sequences among three groups. **B** Hierarchical cluster analysis of miRNA expression in COS rat and natural cycle. On the upper left corner have marked separation based on the miRNA profiling. The expression intensity of each miRNA in each sample varies from high (red) to low (blue). **C** Pathway analysis of target genes of key miRNAs. KEGG pathway analysis showed that the metabolic pathways involved the most target genes. **D** GO analysis of target genes of 30 key miRNAs. It covers 3 parts: biological process, cellular component, and molecular function. The number of genes was shown by grey bars

miR-223-3p Promotes HTR-8/Svneo Cells' Implantation Ability

Since rno-miR-223-3p demonstrated the most prominent difference among three groups in the validation experiment, we selected it for cell siRNA transient transfection and subsequent functional experiments in vitro. We observed that the number of clones and the abilities of invasion, migration, and adhesion were enhanced in the mimic group compared to the NC group, although the difference was not statistically significant. In contrast to the NC and mimic groups, the clone count, invasion, migration, and adhesion abilities of the inhibitor group were significantly reduced compared to group mimic and NC. Consequently, we propose that rno-223-3p is positively correlated with the implantation capacity of HTR-8/Svneo cells.

Discussion

After fertilization, a series of complex procedures after further pregnant preliminarily building is required. The embryo immersed within the UF, which consists of endometrium secretion, fallopian liquid, and serum exudation, connecting the mother and embryo as a kind of “liquid communication medium,” playing key roles in the recognition and establishment of early pregnancy [25]. The volume and ion

concentration of UF during implantation were adjusted by endometrial secretion and absorption, manifesting a “uterine fluid absorption peak” at a crucial time [26]. Meanwhile, contents of UF, such as protein and nucleic acid molecules, are dynamically modified to facilitate timely maternal–fetal interface information exchange [6].

Nowadays, EVs have already been known as a new form of intercellular communication besides paracrine, autocrine, and distant secretion [27]. As previously mentioned, EVs can be generally classified into three subgroups. Exosome, with homogeneous size of 30–150 nm, originates from intracellular multivesicular bodies (MVBs) that fuse with the cell membrane and release. MVs, on the other hand, are directly released by budding from the cell, resulting in an uneven size ranging 100–1000 nm. Both exosomes and MVs can transfer the biological informatic molecule of the original cell to receipt cells and tissues [28]. Among the molecular cargoes in EVs, miRNA is particular importance. These noncoded small RNAs with length of approximately 18–25 nt long and highly conserved across species and play a vital role in regulating a series of physiological functions, including follicular development, oocyte maturation, embryo implantation, and ER in a series of physiological function [29–31]. During implantation, miRNAs can bidirectionally modulate the endometrium and embryo through signaling pathways like Wnt and ERK/MAPK [32–34]. After OS, miRNA expression in the endometrium changes [35].

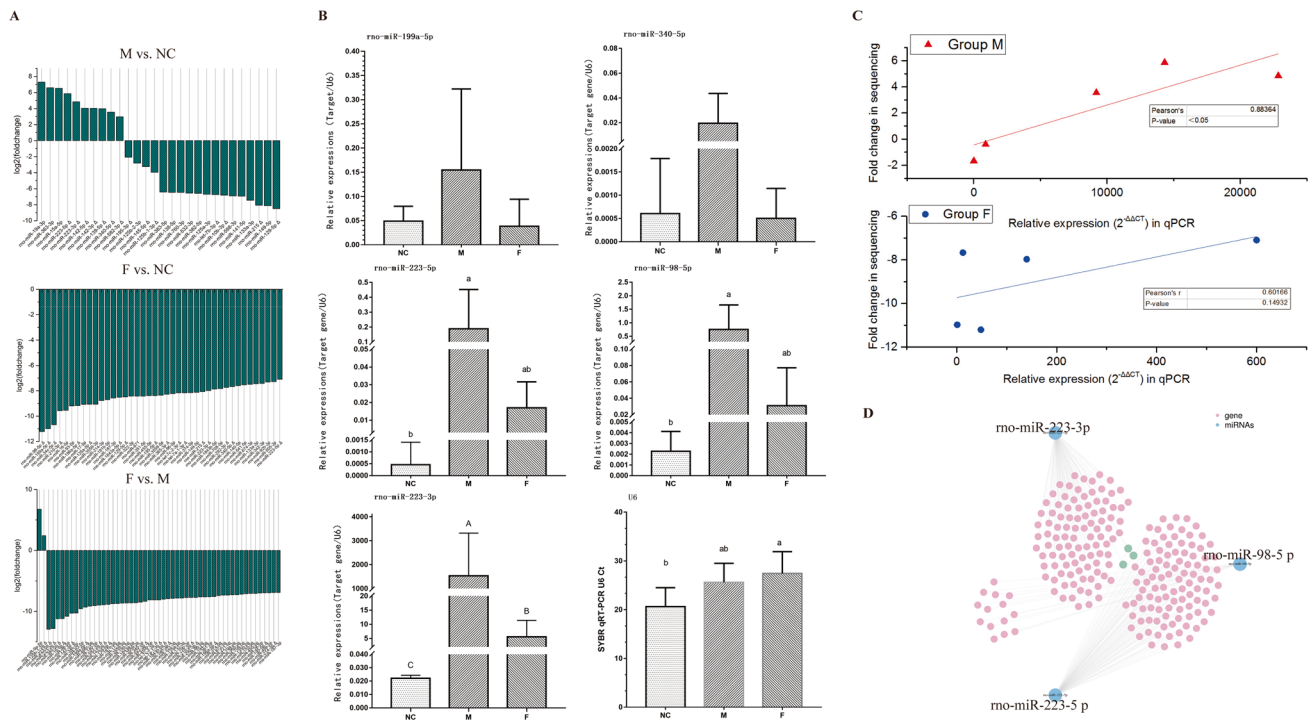


Fig. 4 Key miRNAs validation. **A** Different expression miRNAs among three groups. miRNA was selected according to P -value < 0.05 , fold change > 2 and ranked along with fold change. Key miRNAs marked with Δ . Group M vs. group NC: 10 miRNAs upregulated in group M compared group NC and 11 miRNAs down-regulated; group F vs group NC: 47 miRNAs were downregulated in group F; group F vs group M: 2 miRNAs upregulated and 54 miRNAs downregulated. **B** Expression of rno-miR-223-3p, rno-miR-223-5p, rno-miR-340-5p, rno-miR-98-5p, and rno-miR-199a-5p in

the UF EVs in OS rat and natural cycle were qRT-PCR validated. **C** Group NC was set as the control group and Pearson correlation coefficient was used to assess the correlation between qPCR validation results with relative expression and the sequencing results with fold change. Group M showed a significant correlation while group F not. **D** Target genes network map of miR-223-5p, miR-223-3p, and miR-98-5p and there were only three common target genes: Ankrd17, Col13a1, and Stk39

Thanks to the protection provided by EVs, miRNA inside can be safely transported to target cells or tissues to execute their biological functions. Therefore, the combination of UF, EVs, and miRNAs could act as a cell–cell conversation, diagnostic or prognosis markers, and drug carrier, and could possibly be a new-found way of regulating implantation.

UF EVs, also known as the uterosomes, were firstly reported in the female mammal reproductive fluid in 2008 [7], in which it could transfer the GPI-linked protein to the sperm in mice. In 2013, EVs were first isolated from human UF and the culture medium of endometrial epithelial cell (EECs) [36]. The presence of surface proteins CD63 and CD9 on both EVs and endometrial glands during the proliferative and mid-secretory phase, supporting the hypothesis that UF EVs could be secreted from the endometrium. By comparing miRNA expression between EVs from EECs and their culture medium. The research found a total of 227 miRNA and 13 miRNAs exclusive to EVs. Among them, hsa-mir-200c, hsa-miR-17, and hsa-mir-200c were the most abundant and involved in the adhesion, extracellular matrix receptor signaling pathway, and VEGF-signaling pathway,

which were highly correlated with embryo implantation. Moreover, ovine UF EVs were found to transfer JSRVs to HEK-293 cells [37]. In our study, EVs were successfully isolated from rat UF during implantation, revealing both exosomes and MVs, consistent with previous studies from various species [25, 36].

In our study, we firstly described the alteration of UF EV miRNA expression after the OS treatment in rats. Different protocols and drugs in the OS cycle may bring distinct effects. Several clinical researches indicated that a combination of FSH and LH achieved more follicles but not better pregnancy rate [38–40]. In our study, in a long protocol GnRH agonist, HP-hMG stimulation rats were related with pinopode development state and UF EV miRNA expression that more closely resembled to that in unstimulated, while u-FSH showed a “shut-down” WOI and diverse miRNAs. However, abnormal embryonic implantation occurred in both OS groups, and group M did not yield a greater number of embryos. Therefore, these candidate miRNAs might modulate the receptive ability of endometrium besides WOI on–off.

MiR-223 is located on chromosome X and acts as a network regulatory center, participating in the proliferation and differentiation [41], but its role in reproduction has not yet been fully clarified, and its influences remain uncertain. For instance, miR-223 was highly expressed in ectopic pregnant embryo [42]; UF EV miRNA-223 is more highly expressed in a pregnant sheep [25]; miR-223 in the uterus of PCOS rat decreased and might regulate ER through multiple signaling pathways, such as insulin secretion, Wnt, AMPK, PI3K, and RAS [43]; when endometrial miR-223 is upregulated, LIF and implantation rate decreased in mice [44]; dexamethasone might disrupt ER by valuating the expression of miRNA 223-3p [45].

Target genes of miR-223-3P, miR-223-5p, and miR-98-5P were searched and found three common genes: Ankrd17, Col13a1, and Stk39 (Fig. 4C). Among them, Ankrd17 had the highest expression level in the endometrium. Ankrd17 is an ankyrin family. It is continuously expressed in endometritis cows granulosa cells and reduced the fertility [46] and could also co-activate the HIPPO pathway [47, 48], thereby affecting the proliferation and differentiation of the endometrial epithelium.

Based on the validation experiment, we assumed that UF EV miR-223-3p serves as an essential information carrier and an important molecule involved in the implantation process, therefore rendering it a potential noninvasive biomarker of ER. Subsequently, we study the influences of miR-223-3p on HTR-8/Svneo trophoblast cells' implantation ability. The results revealed a positive effect of miR-223-3p on HTR-8/Svneo cell growth and invasion, migration, and adhesion abilities. Regrettably, the exact origin or target of UF EV miRNA-223 cannot be determined because vesicles of embryonic origin were not strictly eliminated. In our research, we assumed that UF EVs were mostly originated from the endometrium and transferred miR-223-3p to the embryo. Analogous to the diverse differentiation outcomes regulated by miRNA-223 during hematopoiesis processes [41], UF EVs miRNAs were also hypothesized to have effector regions. Up- and downregulation of key miRNAs might damage implantation, but in different ways and with different action thresholds. Moreover, UF EVs transfer proteins, MEP1B for example, to trophoblast cells and promote their proliferation and migration, which provided evidence that UF EVs could be the potential nanomaterials in promoting embryo implantation [13]. miR-223-3p in UF EVs might also be exploited in the future as a therapeutic approach to promote embryo implantation (Fig. 5).

This study is subject to certain constraints. The OS pseudopregnancy animal model can be constructed by ligation of maternal rat to exclude embryonic-derived EVs, further elucidating the role of endometrial-secreted EVs in UF. The study did not directly prove that miR-223-3p plays a role through EV delivery to HTR-8/Svneo cells, an aspect that

can be further explored in future. The isolation efficiency and purity of UF EVs, due to the limited sample size, were unstable. The cryopreservation process might have degraded EV miRNA, which could lead to discrepancies between qRT-PCR validation results and sequencing.

Conclusion

The study firstly analyzed UF EV miRNA sequencing of OS rat, consolidated the reproductive data of EV, and we discovered that UF EV miRNA-3p promotes HTR-8/Svneo cells implantation ability. UF EVs miR-223-3p may be a potential ER noninvasive biomarker during implantation. However, the sequencing and biological function information of UF EVs miRNAs in building early pregnancy is far from adequate to date. Further experiments should be conducted to understand their exact biological functions.

Abbreviations ART: Artificial reproduction technology; ER: Endometrial receptivity; WOI: Window of implantation; OS: Ovarian stimulation; UF: Uterine fluid; EV: Extracellular vesicles; MV: Microvesicles; SD rat: Sprague–Dawley rat; TEM: Transmission electron microscopy; DLS: Dynamic light scattering; qRT-PCR: Quantitative reverse transcription–polymerase chain reaction; GnRH-a: Gonadotropin-releasing hormone agonist; HP-hMG: High-purity human menopausal gonadotropin; U-FSH: Urine follicle stimulation hormone

Supplementary Information The online version contains supplementary material available at <https://doi.org/10.1007/s43032-023-01448-w>.

Acknowledgements The authors appreciate the technical expertise of the team led by Professor Wu of the Lab of Biomedical Electronic Microscopy Higher Research Center, Central South University, Central South University. We would also like to thank everyone in the Reproductive Medicine Center, Xiangya Hospital, Central South University, Changsha, Hunan, People's Republic of China, for their kind help and encouragement.

Author Contribution Y.L. was involved in study concept and supervised the project. X. H. was involved in study design, performing all experiments, data analysis, and writing manuscript. L. X. was involved in experiments. J. Z., Q. Z., and Y. W. provided experiments guide and revised manuscript and figures. All the authors listed have approved the manuscript that is enclosed and agreed to the order of authors.

Data Availability The original data presented in the study are included in the article/supplementary material. Further inquiries can be directed to the corresponding authors.

Declarations

Ethical Approval All experiments were approved by the Institutional Animal Care and Use Committee of Central South University (animal ethics number: 2020sydw0136) and were conducted in accordance with the National Institute for Health Guide for Care and Use of Laboratory Animal.

Conflict of Interest The authors declare no competing interests.

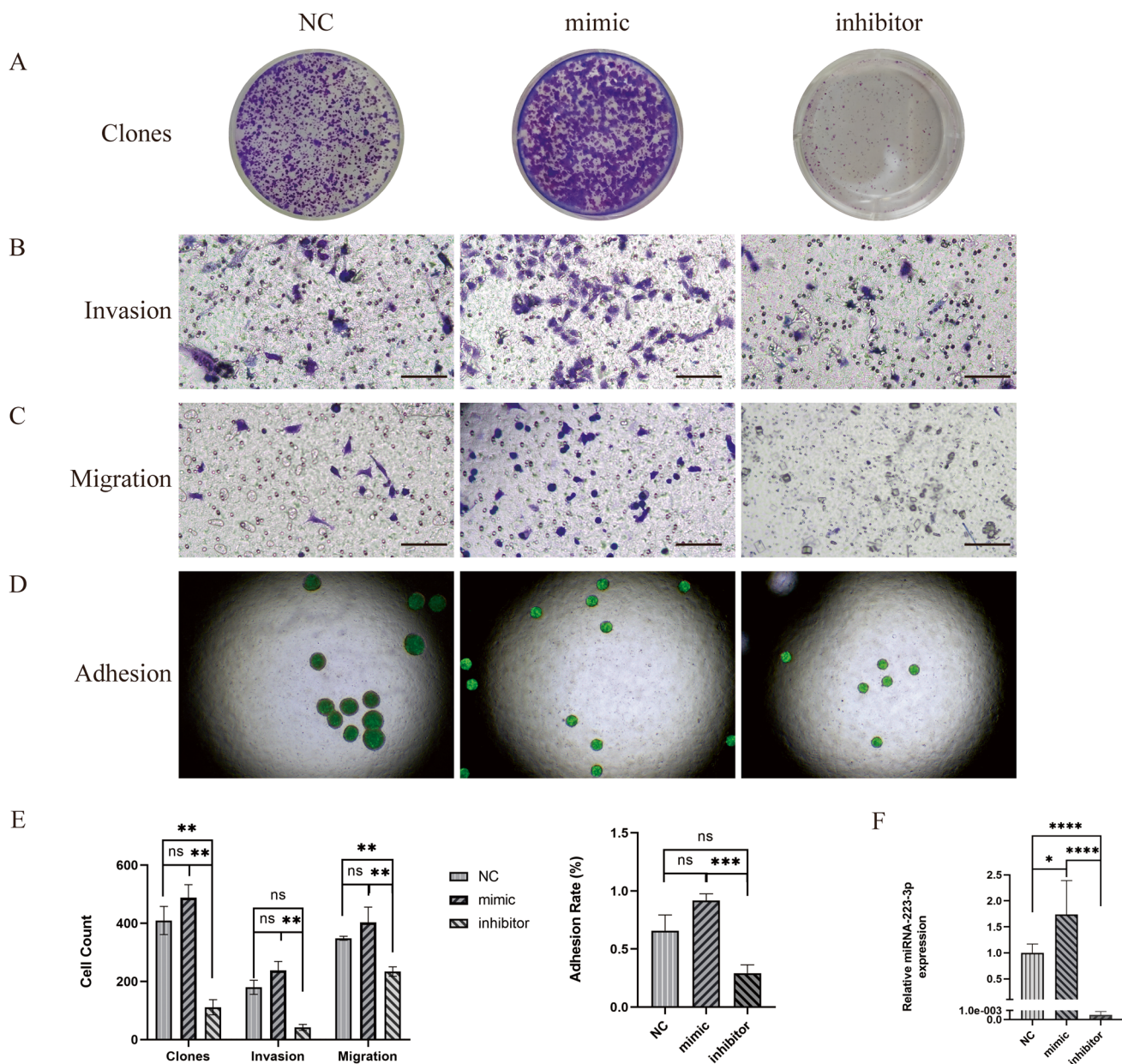


Fig. 5 miR-223-3p might promote HTR-8/Svneo cell growth, invasion, migration, and adhesion. **A** The clones of group mimic were significantly greater than that in group inhibitor. **B** and **C** were invasion and migration assays, group mimic showed better movement

than inhibitor. **D** The ability of adhesion was significantly decreased in group inhibitor. **E** The cell counts of clones, invasion and migration, and the adhesion rate of siRNA HTR-8/Svneo cells were compared. **F** SiRNA was successfully infected into HTR-8/Svneo cells

References

1. Psychoyos A. Uterine receptivity for nidation. *Ann NY Acad Sci.* 1986;476:36–42.
2. Troncoso C, Bosch E, Rubio C, Remohí J, Simón C, Pellicer A. The origin of biochemical pregnancies: lessons learned from pre-implantation genetic diagnosis. *Fertil Steril.* 2003;79:449–50.
3. Chen C, Yan Q, Liu K, Zhou X, Xian Y, Liang D, et al. Endometrial receptivity markers in mice stimulated with raloxifene versus clomiphene citrate and natural cycles. *Reprod Sci.* 2016;23:748–55.
4. Zapantis G, Szymga MJ, Rybak EA, Meier UT. Premature formation of nucleolar channel systems indicates advanced endometrial maturation following controlled ovarian hyperstimulation. *Hum Reprod.* 2013;28:3292–300.
5. Wu JL, Keller P, Kanchwala M, Xing C, Babayev SN, Carr BR, et al. Controlled ovarian stimulation protocols alter endometrial histomorphology and gene expression profiles. *Reprod Sci.* 2020;27:895–904.
6. Zhang Y, Wang Q, Wang H, Duan E. Uterine fluid in pregnancy: a biological and clinical outlook. *Trends Mol Med.* 2017;23:604–14.

7. Griffiths GS, Galileo DS, Reese K, Martin-DeLeon PA. Investigating the role of murine epididymosomes and uterosomes in GPI-linked protein transfer to sperm using SPAM1 as a model. *Mol Reprod Dev.* 2008;75:1627–36.
8. Pan BT, Teng K, Wu C, Adam M, Johnstone RM. Electron microscopic evidence for externalization of the transferrin receptor in vesicular form in sheep reticulocytes. *J Cell Biol.* 1985;101:942–8.
9. Capalbo A, Ubaldi FM, Cimadomo D, Noli L, Khalaf Y, Farcomeni A, et al. MicroRNAs in spent blastocyst culture medium are derived from trophectoderm cells and can be explored for human embryo reproductive competence assessment. *Fertil Steril.* 2016;105:225–235.e3.
10. Fereshteh Z, Bathala P, Galileo DS, Martin-DeLeon PA. Detection of extracellular vesicles in the mouse vaginal fluid: their delivery of sperm proteins that stimulate capacitation and modulate fertility. *J Cell Physiol.* 2019;234:12745–56.
11. Homer H, Rice GE, Salomon C. Review: Embryo- and endometrium-derived exosomes and their potential role in assisted reproductive treatments—liquid biopsies for endometrial receptivity. *Placenta.* 2017;54:89–94.
12. Vojtech L, Woo S, Hughes S, Levy C, Ballweber L, Sauteraud RP, et al. Exosomes in human semen carry a distinctive repertoire of small non-coding RNAs with potential regulatory functions. *Nucleic Acids Res.* 2014;42:7290–304.
13. Hong L, Zang X, Hu Q, He Y, Xu Z, Xie Y, et al. Uterine luminal-derived extracellular vesicles: potential nanomaterials to improve embryo implantation. *J Nanobiotechnol.* 2023;21:79.
14. Abou-Kheir W, Barrak J, Hadadeh O, Daoud G. HTR-8/SVneo cell line contains a mixed population of cells. *Placenta.* 2017;50:1–7.
15. Nishida M. The Ishikawa cells from birth to the present. *Hum Cell.* 2002;15:104–17.
16. Thie M, Denker H-W. In vitro studies on endometrial adhesiveness for trophoblast: cellular dynamics in uterine epithelial cells. *CTO.* 2002;172:237–52.
17. Occhipinti G, Giulietti M, Principato G, Piva F. The choice of endogenous controls in exosomal microRNA assessments from biofluids. *Tumor Biol.* 2016;37(9):11657–65.
18. Livak KJ, Schmittgen TD. Analysis of relative gene expression data using real-time quantitative PCR and the 2- $\Delta\Delta$ CT Method. *Methods.* 2001;25:402–8.
19. Nikas G, Aghajanova L. Endometrial pinopodes: some more understanding on human implantation? *Reprod Biomed Online.* 2002;4:18–23.
20. Hsu C-Y, Hsieh T-H, Tsai C-F, Tsai H-P, Chen H-S, Chang Y, et al. miRNA-199a-5p regulates VEGFA in endometrial mesenchymal stem cells and contributes to the pathogenesis of endometriosis: miRNA99a-5p in endometriosis. *J Pathol.* 2014;232:330–43.
21. Huang K, Dong X, Sui C, Hu D, Xiong T, Liao S, et al. MiR-223 suppresses endometrial carcinoma cells proliferation by targeting IGF-1R. *Am J Transl Res.* 2014;6:841–9.
22. Wang M, Ji S, Shao G, Zhang J, Zhao K, Wang Z, et al. Effect of exosome biomarkers for diagnosis and prognosis of breast cancer patients. *Clin Transl Oncol.* 2018;20:906–11.
23. Xia H-F, Jin X-H, Cao Z-F, Shi T, Ma X. MiR-98 is involved in rat embryo implantation by targeting Bcl-xl. *FEBS Lett.* 2014;588:574–83.
24. Théry C, Witwer KW, Aikawa E, Alcaraz MJ, Anderson JD, Andriantsitohaina R, et al. Minimal information for studies of extracellular vesicles 2018 (MISEV2018): a position statement of the International Society for Extracellular Vesicles and update of the MISEV2014 guidelines. *J Extracell Vesicles.* 2018;7(1):1535750. Available from: <https://www.ncbi.nlm.nih.gov/pmc/articles/PMC6322352/>. Cited 2020 Nov 15.
25. Burns G, Brooks K, Wildung M, Navakanitworakul R, Christenson LK, Spencer TE. Extracellular vesicles in luminal fluid of the ovine uterus. Ye X, editor. *PLoS One.* 2014;9:e90913.
26. Chen Q, Zhang Y, Elad D, Jaffa AJ, Cao Y, Ye X, et al. Navigating the site for embryo implantation: biomechanical and molecular regulation of intrauterine embryo distribution. *Mol Aspects Med.* 2013;34:1024–42.
27. Machtinger R, Laurent LC, Baccarelli AA. Extracellular vesicles: roles in gamete maturation, fertilization and embryo implantation. *Hum Reprod Update.* 2016;22:182–93.
28. Syn NL, Wang L, Chow EK-H, Lim CT, Goh B-C. Exosomes in cancer nanomedicine and immunotherapy: prospects and challenges. *Trends Biotechnol.* 2017;35:665–76.
29. Cretoiu D, Xu J, Xiao J, Suci N, Cretoiu SM. Circulating microRNAs as potential molecular biomarkers in pathophysiological evolution of pregnancy. *Dis Markers.* 2016;2016:3851054.
30. Shekibi M, Heng S, Nie G. MicroRNAs in the regulation of endometrial receptivity for embryo implantation. *Int J Mol Sci.* 2022;23:6210.
31. Liang J, Wang S, Wang Z. Role of microRNAs in embryo implantation. *Reprod Biol Endocrinol.* 2017;15:90.
32. Altmäe S, Martínez-Conejero JA, Esteban FJ, Ruiz-Alonso M, Stavreus-Evers A, Horcajadas JA, et al. MicroRNAs miR-30b, miR-30d, and miR-494 regulate human endometrial receptivity. *Reprod Sci.* 2013;20:308–17.
33. Cuman C, Van Sinderen M, Gantier MP, Rainczuk K, Sorby K, Rombauts L, et al. Human blastocyst secreted microRNA regulate endometrial epithelial cell adhesion. *EBioMedicine.* 2015;2:1528–35.
34. Kropp J, Salih SM, Khatib H. Expression of microRNAs in bovine and human pre-implantation embryo culture media. *Front Genet.* 2014;5:91.
35. Mirkin S, Nikas G, Hsiu J-G, Díaz J, Oehninger S. Gene expression profiles and structural/functional features of the peri-implantation endometrium in natural and gonadotropin-stimulated cycles. *J Clin Endocrinol Metab.* 2004;89:5742–52.
36. Ng YH, Rome S, Jalabert A, Forterre A, Singh H, Hincks CL, et al. Endometrial exosomes/microvesicles in the uterine micro-environment: a new paradigm for embryo-endometrial cross talk at implantation. Ward WS, editor. *PLoS One.* 2013;8:e58502.
37. Kusama K, Nakamura K, Bai R, Nagaoka K, Sakurai T, Imakawa K. Intrauterine exosomes are required for bovine conceptus implantation. *Biochem Biophys Res Commun.* 2018;495:1370–5.
38. Ararooti T, Niasari-Naslaji A, Asadi-Moghaddam B, Razavi K, Panahi F. Superovulatory response following FSH, eCG-FSH and hMG and pregnancy rates following transfer of hatched blastocyst embryos with different diameter and shape in dromedary camel. *Theriogenology.* 2018;106:149–56.
39. Moro F, Scarinci E, Palla C, Romani F, Familiari A, Tropea A, et al. Highly purified hMG versus recombinant FSH plus recombinant LH in intrauterine insemination cycles in women ≥ 35 years: a RCT. *Hum Reprod.* 2015;30:179–85.
40. Tabata C, Fujiwara T, Sugawa M, Noma M, Onoue H, Kusumi M, et al. Comparison of FSH and hMG on ovarian stimulation outcome with a GnRH antagonist protocol in younger and advanced reproductive age women. *Reprod Med Biol.* 2015;14:5–9.
41. Haneklaus M, Gerlic M, O'Neill LAJ, Masters SL. miR-223: infection, inflammation and cancer. *J Intern Med.* 2013;274:215–26.
42. Dominguez F, Moreno-Moya JM, Lozoya T, Romero A, Martínez S, Monterde M, et al. Embryonic miRNA profiles of normal and ectopic pregnancies. *PLoS One.* 2014;9:e102185.
43. Li C, Chen L, Zhao Y, Chen S, Fu L, Jiang Y, et al. Altered expression of miRNAs in the uterus from a letrozole-induced rat PCOS model. *Gene.* 2017;598:20–6.
44. Dong X, Sui C, Huang K, Wang L, Hu D, Xiong T, et al. MicroRNA-223-3p suppresses leukemia inhibitory factor expression and pinopodes formation during embryo implantation in mice. *Am J Transl Res.* 2016;8(2):1155–63.

45. Shariati MBH, Niknafs B, Seghinsara AM, Shokrzadeh N, Ali-vand MR. Administration of dexamethasone disrupts endometrial receptivity by alteration of expression of miRNA 223, 200a, LIF, Muc1, SGK1, and ENaC via the ERK1/2-mTOR pathway. *J Cell Physiol.* 2019;234:19629–39.
46. Piersanti RL, Horlock AD, Block J, Santos JEP, Sheldon IM, Bromfield JJ. Persistent effects on bovine granulosa cell transcriptome after resolution of uterine disease. *Reproduction.* 2019;158:35–46.
47. Zhu H-Y, Ge T-X, Pan Y-B, Zhang S-Y. Advanced role of Hippo signaling in endometrial fibrosis: implications for intrauterine adhesion. *Chin Med J (Engl).* 2017;130:2732–7.
48. Sansores-Garcia L, Atkins M, Moya IM, Shahmoradgoli M, Tao C, Mills GB, et al. Mask is required for the activity of the Hippo pathway effector Yki/YAP. *Curr Biol.* 2013;23:229–35.

Publisher's Note Springer Nature remains neutral with regard to jurisdictional claims in published maps and institutional affiliations.

Springer Nature or its licensor (e.g. a society or other partner) holds exclusive rights to this article under a publishing agreement with the author(s) or other rightsholder(s); author self-archiving of the accepted manuscript version of this article is solely governed by the terms of such publishing agreement and applicable law.